JOURNAL OF PROPULSION AND POWER
Vol. 25, No. 5, September–October 2009

# Scaling and Evaluation of $Pt/Al_2O_3$ Catalytic Reactor for Hydrogen Peroxide Monopropellant Thruster

Sungyong An* and Sejin Kwon†
*Korea Advanced Institute of Science and Technology, Daejeon 305-701, Republic of Korea*

DOI: 10.2514/1.40822

**A scaling methodology of hydrogen peroxide monopropellant thruster is described. As the decomposition process of the hydrogen peroxide on the surface of catalyst bed is extremely complex, empirical method was taken for design purposes. A small-scale thruster was fabricated and important design parameters, including temperature at different locations of the catalyst bed, were measured. Based on the measurement, the catalyst bed size as a function of the propellant flow rate was estimated. Using the scaling methodology, a catalyst bed configuration for a thruster capable of delivering 50 N was estimated. The thruster built on this design produced 42 N at sea level and specific impulse of 123 s.**

## Nomenclature

| | | |
|---|---|---|
| $A_t$ | = | throat area, $cm^2$ |
| $C^*$ | = | characteristic velocity, m/s |
| $C^*_{\text{exp}}$ | = | experiment characteristic velocity, m/s |
| $C^*_{\text{the}}$ | = | theoretical characteristic velocity, m/s |
| $G$ | = | mass flux, $(g/s)/cm^3$ |
| $I_{\text{sp}}$ | = | specific impulse, s |
| $\dot{m}$ | = | mass flow rate of the propellant, g/s |
| $P_c$ | = | pressure inside the reaction chamber, bar |
| $T$ | = | temperature, K |
| $\eta_{C^*}$ | = | efficiency of the characteristic velocity, % |
| $\eta_T$ | = | decomposition efficiency based on the temperature of product gases, % |

## I. Introduction

MONOPROPELLANT propulsion systems have the advantages of liquid-propellant propulsion and less complexity compared with bipropellant systems. Monopropellant systems are widely used for the reaction control system (RCS) of satellites or space launch vehicles, and the weight of the propulsion system is very important.

The use of monopropellant for RCS dates back to the 1940s. Hydrogen peroxide was selected as a propellant for attitude control in projects SYNCOM, Early Bird satellite, X-1 and X-15 experimental aircraft, and the Scout space launch vehicle [1,2]. Hydrogen peroxide had been replaced by hydrazine because of a 20–30% lower specific impulse. Hydrazine thruster has become standard for RCS [3] in spite of high toxicity and potential carcinogenicity.

Interest in rocket-grade hydrogen peroxide was renewed in the mid-1990s as a nontoxic alternative to rocket propellants [1]. Recent studies have investigated rocket-grade hydrogen peroxide as a monopropellant thruster [4–6], a propulsion system for satellites [7,8], a gas generator with dual catalyst bed [9], and catalysts for decomposition of the propellant [10–17] and to investigate long-term storage characteristics [18].

Presented as Paper 5109 at the 44th AIAA/ASME/SAE/ASEE Joint Propulsion Conference and Exhibit, Hartford, CT, 21–23 July 2008; received 6 September 2008; revision received 22 April 2009; accepted for publication 10 June 2009. 

*Ph.D. Candidate, Research Assistant, Division of Aerospace, 373-1 Guseong-dong, Yuseong-gu; kslv@kaist.ac.kr. Student Member AIAA.

†Professor, Division of Aerospace, 373-1 Guseong-dong, Yuseong-gu; trumpet@kaist.ac.kr. Member AIAA.

A thruster consists of injector, reactor including catalyst bed, and nozzle. The reactor is a key component, because the performance of the thruster mainly depends on the catalytic reaction inside the reactor and the size of the catalyst bed. As the decomposition process of the hydrogen peroxide on the surface of catalyst is extremely complex, an empirical method was taken for design purposes. A small-scale test reactor of 1 cm in diameter and 4 cm in length was prepared and tested. The objective of a small-scale test reactor was to obtain the design data that are needed to determine the optimum size of the reactor for a bigger thruster. A larger thruster was designed using the scaling methodology based on the experimental data obtained from the small-scale test reactor. To validate the design procedure, the thruster was built and tested.

## II. Propellant and Catalyst

### A. Propellant

Hydrogen peroxide concentration diluted with water is determined by weight fraction between hydrogen peroxide and water. Decomposition of hydrogen peroxide (100 wt%) into catalysts is described in Eq. (1). The products of the adiabatic exothermic decomposition are completely in gaseous phase only if $H_2O_2$ concentration is more than 67 wt%, due to heat of vaporization of water in the reaction product. The 90 wt% concentrated hydrogen peroxide as a monopropellant from peroxide propulsion was used for the thruster study. The quality of the propellant was in accordance with the requirements of MIL-16005F [19], which defined the maximum allowable impurities for rocket-grade hydrogen peroxide. The propellant density was 1392 $kg/m^3$ at 20°C. Theoretical adiabatic temperature and characteristic velocity were 749°C and 936 m/s, respectively, from the CEA code [20]:

$$H_2O_2\ (\text{liquid}) \rightarrow H_2O\ (\text{gas}) + \tfrac{1}{2}O_2\ (\text{gas}) + \text{heat} \qquad (1)$$

### B. Catalyst Preparation

Platinum was selected as an active material for decomposition of hydrogen peroxide because of its superior reactivity [9]. The catalyst bed was prepared from a $\gamma$-type bimodal alumina pellet from Alfa Aesar that has a size of 1/16 in., a surface area of 255 $m^2/g$, total pore volume of 1.14 $cm^3/g$, and median pore size of 70 $\mu$m and 5000 Å (bimodal type). The preparation was performed with $H_2PtCl_6$ solution as a precursor, using the wetness impregnation method. Impregnation was followed by drying (90°C for 12 h), calcination (300°C for 4 h), and $H_2/N_2$ reduction (300°C for 4 h). The catalyst coating process was carried out twice to increase the mass fraction of loaded platinum. After completion of the coating, 23 wt% of active material was deposited on the support. The virgin alumina pellets and platinum coated alumina pellets are shown in Fig. 1.

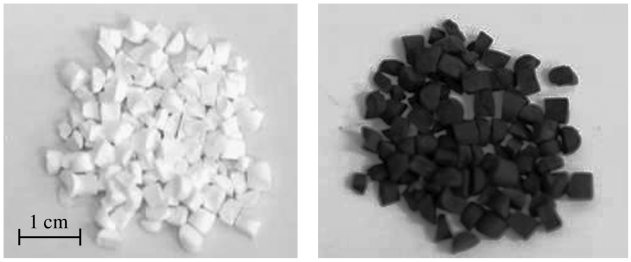


**Fig. 1 Alumina support and prepared catalyst.**

## III. Small-Scale Test Thruster

### A. Design of a Small-Scale Test Reactor

The small-scale test reactor was designed (Fig. 2) and fabricated to evaluate the catalyst bed and to find the decomposition capacity for this catalyst bed [Eq. (2)]. The main components were injector, catalyst bed, and nozzle. An off-the-shelf injector was used to provide homogeneous distribution of the propellant at the front face of the catalyst bed. The Sauter mean diameter of the injected water droplet was 135 $\mu$m, and pressure difference across the injector was 3 bar. The geometry for the reactor was 1 cm in diameter and 4 cm in length, and the catalyst bed was filled in. Six ports were drilled to measure the temperature (T2-5, 1, 2, 3, 4 cm position at catalyst bed from upstream) and pressure (P3-4, before and after catalyst bed) in the reactor:

$$\text{decomposition capacity of catalyst bed} = \frac{\text{propellant mass flowrate g/s}}{\text{catalyst bed volume cm}^3} \tag{2}$$

### B. System Setup and Data Acquisition

The experimental setup was prepared before the thruster test. A schematic of the experimental thruster setup is shown in Fig. 3, which consists of pressurizer nitrogen gas tank, propellant tank, pressure regulation systems, manual valves, solenoid valves, shutoff valve (pneumatic actuator, Swagelok), mass flow meter (AW Company, ACM300, Coriolis type), force sensor (Kistler, 9217A), charge meter (Kistler, 5015A), sliding rail (LM guide), and valve control systems (counter and timer).

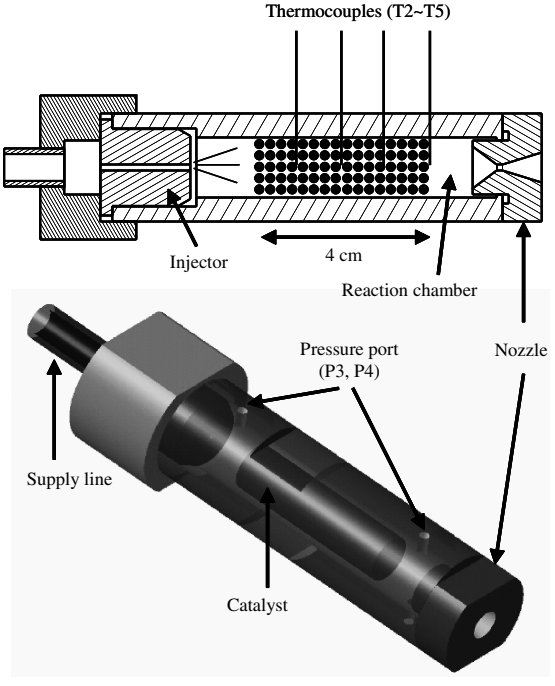


**Fig. 2 Design of the small-scale test thruster.**

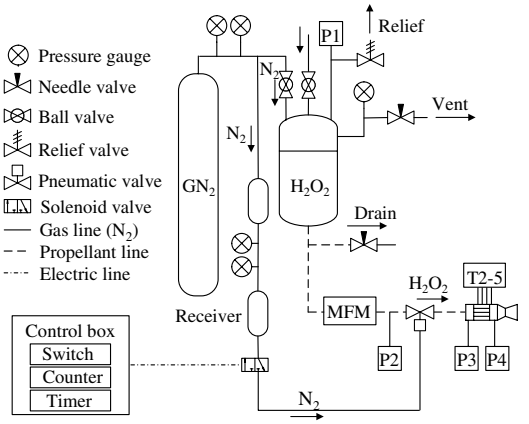


**Fig. 3 Schematic of experimental setup.**

The data acquisition card and SCXI modules with 1 kHz filter from National Instruments for data acquisition were introduced to measure temperature, pressure, thrust force, and propellant mass flow. The sampling rate of data acquisition at the reaction test was 100 samples/s. The K-type thermocouples with an open junction were used for temperature measurement of product gases.

### C. Evaluation Methods

Decomposition efficiency based on the temperature of product gases ($\eta_T$) [Eq. (3)] and efficiency of the characteristic velocity ($\eta_{C^*}$) [Eq. (4)] was used to evaluate the reactor. Adiabatic temperature of the propellant ($T_{\text{adiabatic}}$) and theoretical characteristic velocity ($C^*_{\text{the}}$) were calculated using the CEA code. Temperature of product gases ($T_{\text{product gases}}$), pressure inside the reaction chamber ($P_c$), and propellant mass flow rate ($\dot{m}$) were measured for calculation of two efficiencies. Measurement of thrust force was performed with a load cell and sliding rails, for which the system (including the feeding lines and signal wires) was calibrated before reaction tests, and specific impulse [Eq. (5)] was calculated from thrust data at the final thruster:

$$\eta_T = \frac{T_{\text{product gases}}}{T_{\text{adiabatic}}} \cdot 100 \tag{3}$$

$$\eta_{C^*} = \frac{C^*_{\text{exp}}}{C^*_{\text{the}}} \cdot 100, \qquad C^* = \frac{P_c A_t}{\dot{m}} \tag{4}$$

$$I_{\text{sp}} = \frac{F}{\dot{m} g_0} \tag{5}$$

### D. Results of Reaction Test

A reaction test with a small-scale test thruster was performed to characterize the reactivity of $Pt/Al_2O_3$ catalyst by decomposition efficiency of the propellant based on the temperature of product gases [Eq. (3)]. Temperatures at 1, 2, 3, 4 cm from upstream of the catalyst bed in the reactor were measured. Maximum temperature appeared in the catalyst bed as a function of the propellant mass flow rate (Fig. 4). The position of maximum temperature moved downstream in the reactor with the increase of the propellant mass flow rate. Two regions (A and B) were divided according to whether the fed propellant was fully decomposed or not (Fig. 4). Adiabatic temperature of 90 wt% hydrogen peroxide, 749°C, was obtained at region A, in which the propellant flow rate was lower than region B and fully decomposed. In region B, a maximum temperature was measured at the end of the catalyst bed and observed below adiabatic temperature. Adiabatic temperature was not observed at any position on the catalyst bed in region B.

The efficiency of the characteristic velocity was calculated [Eq. (4)], which is a function of the propellant mass flow rate (Fig. 5). The efficiency was over 90%, which was constant at an increased propellant mass flow rate below 4.0 g/s (region A). Afterward, the

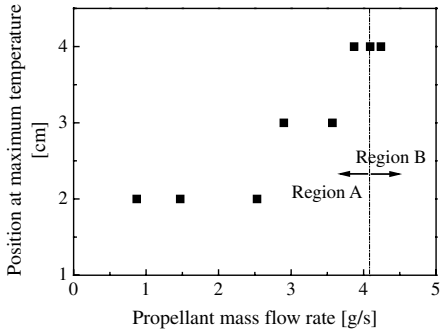


**Fig. 4 Position at maximum temperature on the catalyst bed as a function of the propellant mass flow rate (region A is adiabatic temperature and region B is below adiabatic temperature).**

efficiency considerably decreased with an increase of the propellant mass flow rate over 4.0 g/s (region B). Maximum catalyst capacity [Eq. (2)], which was defined as allowable propellant mass flow rate divided by the volume of the catalyst bed, was 1.27 $(g/s)/cm^3$, as observed at the boundary of regions A and B.

## IV. Scaled-Up Thruster

### A. Design of a Larger Thruster

The small-scale test reactor was scaled up to a 50 N level (Fig. 6), which will be able to fully decompose 33 g/s of 90 wt% hydrogen peroxide. The catalyst bed was 3 cm in diameter and 4 cm in length, determined from experimental data of decomposition capacity of the catalyst bed for the small-scale test reactor. It was scaled up to the radial direction to decompose larger propellant flow rate than the small-scale test reactor (Fig. 7). The scaled-up thruster was evaluated by decomposition efficiency based on the temperature $\eta_T$, efficiency of the characteristic velocity $\eta_{C^*}$, and measurement of thrust force.

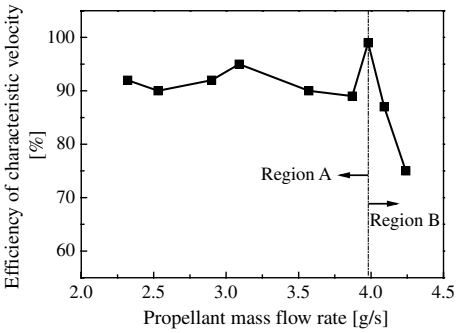


**Fig. 5 Efficiency of the characteristic velocity as a function of the propellant mass flow rate.**

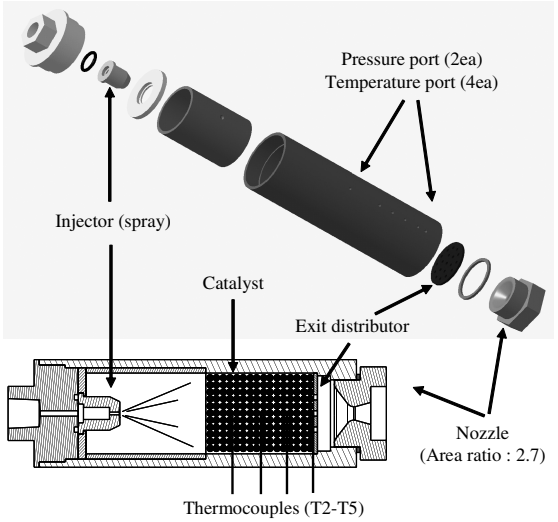


**Fig. 6 Design of the scaled-up thruster.**

### B. Test Results

A reaction test was performed with a scaled-up thruster, using test times of 20 s at continuous mode. The temperature profile at each position during the reaction is shown in Fig. 8. The test was done from a cold start (without heating of the propellant and catalyst bed) at sea level. Propellant mass flow rate was 34.8 g/s, which is enough flow rate to produce 50 N thrust under vacuum conditions. Temperature sharply increased, reaching steady-state value several seconds after the main valve was opened. Adiabatic temperature was observed at the end of the catalyst bed (4 cm position from upstream of the catalyst bed). The decomposition efficiency, based on the temperature of product gases, was about 100%.

Pressure and thrust data are shown in Fig. 9. Propellant feeding pressure was 22.8 bar, and reaction-chamber pressure was 16.2 bar. The efficiency of the characteristic velocity was 98% and full decomposition of 34.8 g/s occurred. The thrust was 42 N, and so specific impulse was calculated as 123 s at sea level. In addition, pressure oscillation inside the reaction chamber was not observed

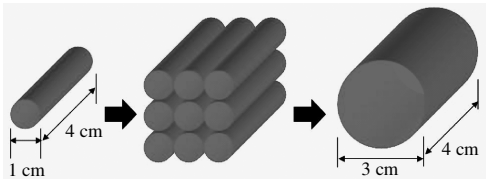


**Fig. 7 Scaled-up concept of the catalyst bed to the radial direction; catalyst for small-scale test thruster (left) and catalyst for scaled-up thruster (right).**

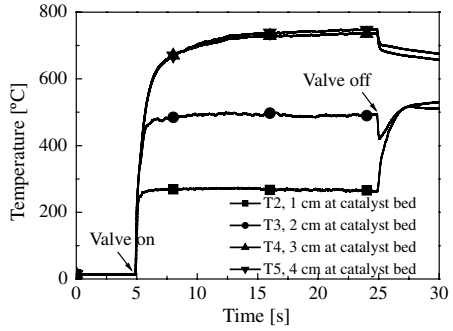


**Fig. 8 Temperature measurement as a function of time at 50 N thruster ($\dot{m} = 34.8$ g/s and $\eta_T = 99.9\%$).**

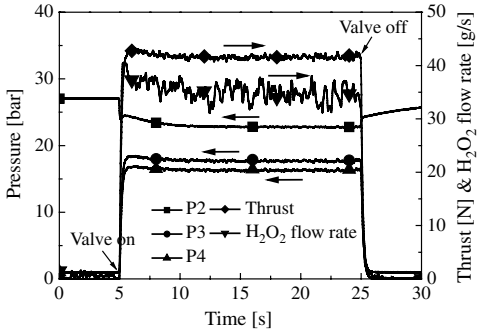


**Fig. 9 Pressure and thrust measurement as a function of time at 50 N thruster ($\dot{m} = 34.8$ g/s and $\eta_{C^*} = 98\%$).**

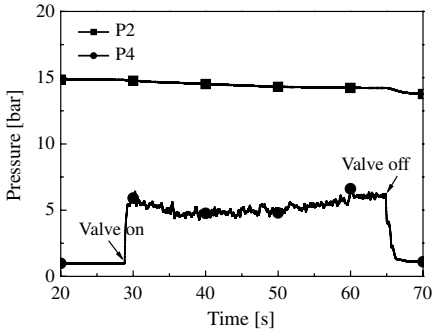


**Fig. 10 Low reaction-chamber pressure at small-scale test thruster ($\dot{m} = 3.9$ g/s and $\eta_{C^*} = 68\%$).**

and was very stable. The pressure drop across the catalyst bed was 1.4 bar.

## V. Conclusions

Silver has been widely used as a catalyst for decomposition of hydrogen peroxide. The melting point of silver is about 960°C. Thus, there was a melting problem in the case of silver during thruster operation with highly concentrated hydrogen peroxide [21]. Manganese oxide is a possible candidate for decomposition of hydrogen peroxide, but it has lower activity than a precious metal catalyst. In addition, it is reported that a manganese oxide catalyst on washcoated cordierite is easily washed out at the reaction test, due to its low adhesion to cordierite [9]. Platinum was selected as an alternative to these active materials to avoid these problems. The melting point of platinum is much higher than the adiabatic temperature of 100 wt% hydrogen peroxide, and its characteristic has been well studied by many chemical researchers. In addition, platinum has been known as a promising candidate to have good reactivity with hydrogen peroxide [22].

The overall size of the thruster mainly depends on the size of the catalyst bed, because all of the fed propellant needs to be decomposed inside the reactor [12]. The thruster is a compact size if the decomposition rate of the propellant on the catalyst bed is high, but bulky if the decomposition capacity of the catalyst bed [Eq. (2)] is low, because a larger catalyst bed is needed for full decomposition of the designed propellant flow rate. Thus, the decomposition capacity of the catalyst bed [Eq. (2)] is a key parameter in designing a thruster for a larger thruster design. The mass flux [Eq. (6)], which is defined as propellant mass flow rate divided by the frontal area of the catalyst bed, usually indicates the decomposition capacity of the catalyst bed [13]. However, mass flux does not represent the total capacity of the catalyst, because information about the length of the catalyst bed is missing:

$$G = \frac{\text{propellant mass flowrate g/s}}{\text{cross-sectional area of reactor cm}^2} = \frac{\dot{m}}{A} \tag{6}$$

The decomposition capacity of the catalyst [(Eq. (2)] instead of mass flux [Eq. (6)] is proposed to more accurately describe the capacity of the catalyst bed. The decomposition rate of the propellant was assumed to be proportional to the volume of the catalyst bed and inversely proportional to the propellant mass flow rate. Catalyst volume, which includes the information of catalyst length, was used in place of the cross-sectional area of the catalyst bed in Eq. (2). Propellant mass flow rate was gradually increased to find the maximum decomposition capacity of the catalyst bed. The pressure inside the reaction chamber was set near 16 bar at all reaction tests by adjusting both the pressure of pressurizer gas and the throat area of nozzle. There are two reasons. The first reason is to prevent the pressure effect. If a high pressure is built up inside the reaction chamber, then the decomposition efficiency increases due to increased residence time of reactant. On the other hand, the decomposition efficiency decreases in the case of low chamber pressure. Figure 10 shows the case of low decomposition efficiency in the case of low chamber pressure. The propellant flow rate was 3.9 g/s, which is still full decomposition flow rate at 16 bar reaction chamber pressure. However, the efficiency of the characteristic velocity was just 68% if the chamber pressure was about 5 bar. Therefore, chamber pressure was fixed to one point to view only: the effect of catalyst activity. The second reason for remaining at 16 bar inside chamber pressure is safety. The reaction test was operated in a low-pressure region because the test was performed at a small laboratory at Korea Advanced Institute of Science and Technology (KAIST), although higher reactivity can be obtained if higher pressure is built up inside the reactor. The maximum decomposition flow rate of the propellant onto the catalyst bed was determined as a point at which the decomposition efficiency was still maximized and started to decrease with increase in the propellant flow rate. The objective of a small-scale test thruster was to obtain the decomposition capacity of the catalyst bed, which was developed at KAIST. The maximum capacity was 1.23 $(g/s)/cm^3$, based on decomposition efficiency of temperature of product gas [Eq. (3)] (Fig. 4) and 1.27 $(g/s)/cm^3$ based on efficiency of the characteristic velocity [Eq. (4)] (Fig. 5). These two values were in agreement.

A scaled-up thruster used the same catalyst as the small-scale test thruster. The size of the catalyst bed was enlarged for full decomposition of the designed flow rate, but with the same value of decomposition capacity of the catalyst bed as the small-scale test thruster. There were two considerations to enlarge the catalytic reactor: one was to increase the reactor in the radial direction and another was to increase the length. That was a design problem. The small-scale test thruster was scaled up in the radial direction to prevent the pressure loss across the catalyst bed from increasing. A verification test of the scaled-up thruster was performed. As a result, almost all of the propellant was decomposed into catalyst. A catalyst bed, 3 cm in diameter and 4 cm in length, had full decomposition at 34.8 g/s (about a flow rate for 50 N at vacuum). A 99.9% temperature efficiency and a 98% efficiency of the characteristic velocity was demonstrated for the scaled-up thruster. The measured specific impulse was 123 s, which is 96% of the theoretical specific impulse at the test condition (sea level and 16 bar chamber pressure). In view of these data, it was concluded that the final thruster was properly designed with the optimum size of the catalyst bed. Catalyst evaluation methodology by defining the decomposition capacity of the catalyst bed and scaled-up procedure of the reactor were effective at enlarging a thruster.

## Acknowledgment

This work was supported by the Korea Science and Engineering Foundation (KOSEF) grant funded by the Korea Ministry of Education, Science and Technology (MEST) through the National Research Laboratory (NRL) (no. R0A-2007-000-20065-0).

## References

[1] Ventura, M., and Mullens, P., "The Use of Hydrogen Peroxide for Propulsion and Power," 35th AIAA/ASME/SAE/ASEE Joint Propulsion Conference and Exhibit, Los Angeles, AIAA Paper 99-2880, 1999.

[2] Love, J. E., and Stillwell, W. H., "The Hydrogen Peroxide Rocket Reaction Control System for the X-1B Research Airplane," NASA TN D-185, 1959.

[3] Kim, J. S., Park, J., and Kim, S., "Test and Performance Evaluation of Small Liquid monopropellant Rocket Engines," 42nd AIAA/ASME/SAE/ASEE Joint Propulsion Conference and Exhibit, Sacramento, CA, AIAA Paper 2006-4388, 2006.

[4] Scharlemann, C., Schiebl, M., Marhold, K., Tajmar, M., Miotti, P., Kappenstein, C., Batonneau, Y., Brahmi, R., and Hunter, C., "Development and Test of a Miniature Hydrogen Peroxide Monopropellant Thruster," 42nd AIAA/ASME/SAE/ASEE Joint Propulsion Conference and Exhibit, Sacramento, CA, AIAA Paper 2006-4550, 2006.

[5] Barley, S., Palmer, P. L., and Coxhill, I., "Evaluating the Miniaturisation of a Monopropellant Thruster," 42nd AIAA/ASME/SAE/ASEE Joint Propulsion Conference and Exhibit, Sacramento, CA, AIAA Paper 2006-4549, 2006.

[6] Pasini, A., Torre, L., Romeo, L., Cervone, A., d'Agostino, L., Musker, A. J., and Saccoccia, G., "Experimental Characterization of a 5 N Hydrogen Peroxide Monopropellant Thruster Prototype," 43rd AIAA/

ASME/SAE/ASEE Joint Propulsion Conference and Exhibit, Cincinnati, OH, AIAA Paper 2007-5465, 2007.

[7] An, S., Lim, H., and Kwon, S., "Hydrogen Peroxide Thruster Module for Microsatellites with Platinum Supported by Alumina as Catalyst," 43rd AIAA/ASME/SAE/ASEE Joint Propulsion Conference and Exhibit, Cincinnati, OH, AIAA Paper 2007-5467, 2007.

[8] Sahara, H., Nakasuka, S., Sugawara, Y., and Kobayashi, C., "Demonstration of Propulsion System for Microsatellite Based on Hydrogen Peroxide in SOHLA-2 Project," 43rd AIAA/ASME/SAE/ASEE Joint Propulsion Conference and Exhibit, Cincinnati, OH, AIAA Paper 2007-5575, 2007.

[9] Lim, H., An, S., Kwon, S., and Rang, S., "Hydrogen Peroxide Gas Generator with Dual Catalytic Beds for Nonpreheating Startup," *Journal of Propulsion and Power*, Vol. 23, No. 5, 2007, pp. 1147–1150. doi:10.2514/1.28897

[10] Pirault-Roy, L., Kappenstein, C., Guerin, M., and Eloirdi, R., "Hydrogen Peroxide Decomposition of Various Supported Catalysts Effect of Stabilizers," *Journal of Propulsion and Power*, Vol. 18, No. 6, 2002, pp. 1235–1241. doi:10.2514/2.6058

[11] Tian, H., Zhang, T., Sun, S., Liang, D., and Lin, L., "Performance and Deactivation of $Ir/\gamma$-$Al_2O_3$ Catalyst in the Hydrogen Peroxide Monopropellant Thruster," *Applied Catalysis A*, Vol. 210, Nos. 1–2, 2001, pp. 55–62. doi:10.1016/S0926-860X(00)00829-2

[12] Kappenstein, C., Pirault-Roy, L., Guerin, M., Wahdan, T., Asma, A. A., Fakhreia A. A., and Mohamed Z. I., "Monopropellant Decomposition Catalysts V. Thermal Decomposition and Reduction of Permanganates as Models for the Preparation of Supported MnOx Catalysts," *Applied Catalysis A*, Vol. 234, Nos. 1–2, Aug. 2002, pp. 145–153. doi:10.1016/S0926-860X(02)00220-X

[13] Ventura, M. C., and Wernimont, E. J., "Advancements in High Concentration Hydrogen Peroxide Catalyst Beds," 37th AIAA/ASME/SAE/ASEE Joint Propulsion Conference and Exhibit, AIAA Paper 2001-3250, 2001.

[14] Rusek, J. J., "New Decomposition Catalysts and Characterization Techniques for Rocket-Grade Hydrogen Peroxide," *Journal of Propulsion and Power*, Vol. 12, No. 3, 1996, pp. 574–579. doi:10.2514/3.24071

[15] Wernimont, E. J., and Durant, D., "State of the Art High Performance Hydrogen Peroxide Catalyst Beds," 40th AIAA/ASME/SAE/ASEE Joint Propulsion Conference and Exhibit, Fort Lauderdale, FL, AIAA Paper 2004-4147, 2004.

[16] Russo Sorge, A., Turco, M., Pilone, G., and Bagnasco, G., "Decomposition of Hydrogen Peroxide on $MnO_2/TiO_2$ Catalysts," *Journal of Propulsion and Power*, Vol. 20, No. 6, 2004, pp. 1069–1075. doi:10.2514/1.2490

[17] Kuan, C.-K., Chen, G.-B., and Chao, Y.-C., "Development and Ground Tests of a 100-Millinewton Hydrogen Peroxide Monopropellant Microthruster," *Journal of Propulsion and Power*, Vol. 23, No. 6, 2007, pp. 1313–1320. doi:10.2514/1.30440

[18] Ventura, M. C., "Long Term Storability of Hydrogen Peroxide," 41st AIAA/ASME/SAE/ASEE Joint Propulsion Conference and Exhibit, Tucson, AZ, AIAA Paper 2005-4551, 2005.

[19] "Propellant, Hydrogen Peroxide," U.S. Dept. of Defense, Performance Specification MIL-PRF-16005F, 2003

[20] Stanford, G., and McBride, B. J., "Computer Program for Calculation of Complex Chemical Equilibrium Compositions and Applications," NASA Ref. Publ. 1311, 1994.

[21] Ahn, S.-H., Choi, T.-H., Krishnan, S., and Lee, C.-W., "A Laboratory Scale Hydrogen-Peroxide Rocket Engine Facility," 39th AIAA/ASME/SAE/ASEE Joint Propulsion Conference and Exhibit, Huntsville, AL, AIAA Paper 2003-4647, 2003.

[22] Romeo, L., Torre, L., Pasini, A., Cervone, A., d'Agostino, L., and Calderazzo, F., "Performance of Different Catalysts Supported on Alumina Spheres for Hydrogen Peroxide Decomposition," 43rd AIAA/ASME/SAE/ASEE Joint Propulsion Conference and Exhibit, Cincinnati, OH, AIAA Paper 2007-5466, 2007.

C. Avedisian
*Associate Editor*